Molecular Self-Assembly at Bare Semiconductor Surfaces: Investigation of the Chemical and Electronic Properties of the Alkanethiolate –GaAs(001) Interface

ARTICLE *in* THE JOURNAL OF PHYSICAL CHEMISTRY C · FEBRUARY 2007

Impact Factor: 4.77 · DOI: 10.1021/jp065173a

5 AUTHORS, INCLUDING:

Amy V Walker
University of Texas at Dallas
60 PUBLICATIONS **1,292** CITATIONS
SEE PROFILE

David L Allara
Pennsylvania State University
261 PUBLICATIONS **23,005** CITATIONS
SEE PROFILE

Molecular Self-Assembly at Bare Semiconductor Surfaces: Investigation of the Chemical and Electronic Properties of the Alkanethiolate−GaAs(001) Interface

Christine L. McGuiness,[†] Andrey Shaporenko,[‡] Michael Zharnikov,[‡] Amy V. Walker,[§] and David L. Allara*[,†]

Departments of Chemistry and Materials Science, The Pennsylvania State University, 104 Chemistry Building, University Park, Pennsylvania 16801-6300, Angewandte Physikalische Chemie, Universität Heidelberg, Im Neuenheimer Feld 253, D-69120 Heidelberg, Germany, and Department of Chemistry, Washington University, Campus Box 1134, Washington University, St. Louis, Missouri 63130

Received: August 10, 2006; In Final Form: January 5, 2007

High-resolution X-ray photoelectron spectroscopy (HRXPS), time-of-flight secondary ion mass spectrometry (ToF-SIMS), and Raman scattering have been used to characterize the bonding and electronic properties of the interfaces formed by ambient-temperature, solution self-assembly of octadecanethiol and dodecanethiol under oxygen-free conditions on GaAs(001) surfaces. The combination of HRXPS and ToF-SIMS shows that both monolayers form direct S−[GaAs] attachment to the bare substrate with dominant As−S bonding and some fraction of Ga−S bonding, but the densely packed octadecanethiolate self-assembled monolayers (SAMs) are significantly more effective in protecting the interface from oxide regrowth compared to the less dense dodecanethiolate SAMs. Raman scattering measurements of the GaAs LO phonon modes indicate that the formation of these direct, oxide-free S−[GaAs] interfaces does not induce any significant changes in the GaAs surface electronic states, whereas control experiments with inorganic sulfide treatment does indicate a significant reduction in the surface traps, consistent with earlier reports. Overall these experiments show that the formation of direct alkane−S−[GaAs(001)] interfaces of high quality provides a method to passivate the GaAs surface against oxide regrowth but does not necessarily lead to changes in the surface electronic states.

1. Introduction

The direct attachment of molecules to oxide-stripped GaAs-(001) surfaces via chalocogenide atoms has been of longstanding interest as a possible means of chemically and electronically passivating the surface for electronic and optoelectronic device applications.[1−3] The early studies, involving sulfur-containing molecules ranging from organosulfides[1,4−9] to short organic thiols,[10−13] demonstrated the feasibility of reducing the barrier height and surface recombination velocity from the undesirable values associated with the problematic native oxide.[1,4,6,7,12−16] In these studies there was no particular attempt to control or characterize the organization and packing density of the molecular films, so structure−property correlations were difficult. More recently, the functionalization of GaAs surfaces has been achieved using organized self-assembled monolayer (SAM) films of alkanethiols[17−25] and aromatic thiols[26−28] for which the structures of the molecular assemblies are reasonably well-defined in terms of a single monolayer and some degree of organization of the molecules attached to the substrate. Dorsten and co-workers reported Raman scattering measurements of octadecanethiol ($C_{18}H_{37}SH$; ODT) SAMs on GaAs-(001) that were interpreted in terms of the electron−phonon coupling in the surface region and concluded that the formation of these SAMs results in some reduction of surface traps with the effects persisting for months.[19] In addition, SAMs of alkanedithiols have been shown to modify Schottky diode device characteristics.[25,29−31]

In most of these cases, however, little definitive information is available on the actual packing and coverages of the molecules and, more importantly, on the presence and detailed character of the chemical binding of the adsorbate molecules to the substrate. Nesher and co-workers, in a study of the electrical characteristics of GaAs−*n*-alkanethiolate−Hg junctions for alkyl chains with $n = 12$, 14, 15, and 18,[25] characterized the SAMs by X-ray photoelectron spectroscopy (XPS) derived thicknesses, liquid drop contact angles, and qualitative chain conformational ordering via infrared reflection spectroscopy. They concluded that for the ODT SAM the chains were densely packed and oriented nearly perpendicular to the surface, in agreement with our earlier report,[24] and detailed the electrical transport properties through the monolayer. Their data, however, do not reveal details on the molecule-mediated modification of the surface electronic properties.

Without these details the effects of the binding on the surface electronic properties cannot be properly understood. Defining the exact types of S−substrate bonds is complicated for the polar (001) surface since there are two surface termination planes, one with Ga and one with As atoms, and each intrinsic surface has two dangling bonds.[32] Further, even under carefully controlled conditions these surfaces have been observed to undergo many different reconstructions,[32,33] some of which can provide both Ga and As binding sites. Finally, from a thermochemical point of view one might expect a preference for S binding to Ga based on thermal annealing experiments[34−36] and predictions[37] that show a preference of inorganic sulfides bonding to the group III atom (Ga). In the first reports of $(NH_4)_2S_x$ ($x \geq 1$) treated GaAs(001) surface, only As−S species were observed from XPS measurements.[38] Subsequent studies

* Corresponding author. E-mail: dla3@psu.edu.
[†] The Pennsylvania State University.
[‡] Universität Heidelberg.
[§] Washington University.

10.1021/jp065173a CCC: $37.00
Published on Web 02/28/2007

with high-resolution photoemission showed evidence for both As−S and Ga−S bonds,[39−42] and more sophisticated surface analysis has revealed a complicated model including an amorphous As−S phase terminated by Ga−S bonds.[43,44] In the cases of organothiols even more discrepancies exist. For example, Lunt et al. did not observe either Ga−S or As−S bonds for any short organic thiol films studied,[12,13] On the other hand, the exclusive presence of Ga−S bonds was proposed for propanethiol and ethanethiol functionalized surfaces[10,11] whereas As−S bonds have been exclusively reported for the cases of SAMs of aromatic thiols,[45,46] alkanethiols,[21,23,25,47] and mercaptosilanes.[48] Both Ga−S bonding and As−S bonding have been reported, however, for films of sulfur-containing peptides.[47] In all cases where As−S bonds have been observed, the native oxide was removed using a wet chemical etch.[7,9,12,21,23,25,38,39,45−48] Both acidic and basic conditions can be used to remove the amphoteric oxide, so that even within this subcategory of oxide removal the resulting surface chemistry can be very different.[49] For example, when the native oxide is removed using NH_4OH, a hydrophilic surface passivated by a small oxide layer is formed,[50,51] little hydrocarbon contamination is observed, and the surface is found to be nearly stoichiometric with only a slight excess of As.[50] In comparison, when the oxide is removed using HCl, a hydrophobic surface results with less surface oxidation but more hydrocarbon contamination. This surface has been noted to be enriched by elemental arsenic.[50−52]

In a recent report we detailed the preparation and characterization of an ODT/GaAs(001) SAM, which to our knowledge is the most reproducible, well-organized organothiolate monolayer on GaAs(001) reported to date.[24] This report showed the alkyl chains to exhibit high conformational ordering with 14°−15° tilts from the surface normal. Initial XPS results showed that the remaining oxide from the preliminary stripping procedure was thoroughly removed during the self-assembly procedure, likely due to a sacrificial "etching" action by solute thiol molecules, to leave an oxide-free (molecule)−[GaAs(001)] interface. The presence of specific As−S and/or Ga−S bonding, however, could not be concluded due to resolution limitations of the XPS instrumentation. Under similar assembly conditions, Nesher et al. reported a similar monolayer structure but suggested that the "alkylthiol binds selectively through As−S bonds"; the remaining Ga atoms were presumed to be bound to oxygen atoms.[25]

Since a detailed understanding of the bonding of the thiol molecules is critical to understanding the behavior of these films, and since our SAMs appear to represent a near-limiting case of a well-defined molecular organization and a direct (molecule)−(substrate) interface, we have continued our investigation of ODT/GaAs(001) SAMs by applying high-resolution XPS (HRXPS) and time-of-flight secondary ion mass spectrometry (ToF-SIMS) measurements to discern in detail the molecule−substrate bonding. In addition, we probe the effect of the alkanethiolate monolayer formation on the electron−hole recombination velocities at the GaAs surface by means of Raman scattering measurements, following the work of Dorsten et al.,[19] and compare our results to well-known Raman scattering measurements of inorganic sulfide treated GaAs surfaces.[16] While the influence of molecular adsorbates on the GaAs surface electronic properties has also been examined with surface photovoltage spectroscopy,[53] photoluminescence,[54] and photoemission[25] experiments, we employ quantitative, confocal, micro-Raman scattering measurements that allow spot-to-spot comparisons across the GaAs surface at high lateral resolutions ($\sim$1 μm).

In this paper we examine the well-organized ODT SAM and, for comparison, the shorter chain dodecanethiol ($C_{12}H_{23}SH$; DDT) SAM, which shows a much lower degree of molecular organization. We find that while both monolayers form a direct thiolate bond to the bare GaAs surface, the ODT SAM is much better at preventing oxide regrowth in the interface under ambient conditions than the DDT SAM. The HRXPS measurements show evidence for the dominant presence of As−S bonding for both ODT and DDT SAMs, while ToF-SIMS measurements indicate that some fraction of Ga−S bonding is present as well. These data are further interpreted in terms of our previous report that the chains, on average, appear to pack in a manner incommensurate with the intrinsic (001) substrate surface lattice. Finally, the Raman scattering spectra of the GaAs LO lattice modes show no evidence for any significant electron−phonon coupling induced intensity shifts upon formation of the SAMs. From these data we conclude that even for the case of the extremely well organized, dense, ODT SAM the presence of the chemically bound molecules has only minor effects on the GaAs surface electronic states.

2. Experimental Methods

2.1. Materials and Monolayer Formation. Octadecanethiol (ODT, $CH_3[CH_2]_{17}SH$), dodecanethiol (DDT, $CH_3[CH_2]_{11}SH$), and $Na_2S\cdot 9H_2O$ were obtained from Aldrich Chemical Co. (Milwaukee, WI) and used as received. Two types of GaAs-(001) substrates were used for monolayer formation: undoped double side polished and single side polished n^+-type doped wafers (Si dopant density (N_e) = 1.1×10^{18} cm^{-3} and 2.7×10^{18} cm^{-3}, American Xtal Technologies, Fremont, CA). The n^+-type GaAs wafers were used for Raman scattering studies; a combination of doped and undoped wafer samples ($\sim 1 \times 1$ cm^2) was used for all other studies. No differences were observed between the SAM properties for doped and undoped wafers.[24]

The optimum procedure for forming high-quality monolayers on GaAs(001) surfaces has already been reported[24] and was used for these experiments. Briefly, the native oxide of GaAs was removed by immersing the substrates in concentrated NH_4OH (J.T. Baker, CMOS grade, 30% NH_4OH in water) from 1 to 5 min. Immediately after immersion, the sample was rinsed with anhydrous ethanol (Pharmco, ACS/USP grade) and dried in a N_2 stream. The substrates were then immersed within 3 min in degassed ethanolic solutions containing 3 mM ODT or DDT and $\sim$10 mM NH_4OH and transferred into a nitrogen-purged glovebox (O_2 < 5 ppm) for incubation for at least 20 h. For the HRXPS and ToF-SIMS measurements, the samples were stored in nitrogen-purged puff bags for 1−7 days before measurements were made. This is less time than the time for the onset of noticeable oxidation of ODT SAMs stored under ambient conditions.[24]

For comparison in Raman scattering experiments, the n^+-type doped GaAs wafers were treated with $Na_2S\cdot H_2O$. This was achieved by spin-coating a 1 M aqueous solution of $Na_2S\cdot H_2O$ on a freshly etched NH_4OH GaAs wafer. This similar to a procedure described previously.[16]

2.2. High-Resolution X-ray Photoelectron Spectroscopy (HRXPS). The HRXPS measurements were carried out at the D1011 beamline of the synchrotron storage ring MAX II at MAX-Lab in Lund, Sweden, at room temperature and a base pressure lower than 1.5×10^{-9} Torr. The spectra (Ga 3d, As 3d, C 1s, O 1s, and S 2p) were collected by a SCIENTA analyzer in normal emission geometry. Excitation energies in the range of 130−580 eV were used. The choice of photon

energy (PE) for a particular spectrum was based on the optimization of the photoionization cross section for the corresponding core level[55−57] and on adjustment of either surface or bulk sensitivity. The spectra acquisition time was selected in such a way that no noticeable damage by the primary X-rays occurred during the measurements.[58−61]

The energy resolution was better than 100 meV, allowing a clear separation of individual spectral components. The energy width of the individual emissions was close to the intrinsic energy spread of the respective core-level photoemission process. Energy calibration was performed individually for every spectrum to avoid effects related to the instability of the monochromator. The binding energy (BE) scale was referenced to the pronounced Au $4f_{7/2}$ "bulk" peak (83.93 eV) of a reference DDT/Au sample,[60,62] which was attached to the same sample holder as the probed one. The value of 83.93 eV was derived from an independent calibration to the Fermi edge of a clean Pt foil. This is close to the value of 83.95 eV given for Au $4f_{7/2}$ by the latest ISO standard.[63]

The decomposition of the HRXPS spectra was performed self-consistently over the entire data set. The spectra were fitted using Voigt peak profiles and a Shirley background. To fit the doublet emissions (Ga 3d, As 3d, and S 2p), we used two peaks with the same full width at half-maximum (fwhm), a reasonable spin−orbit splitting, and branching ratios of 2:1 ($2p_{3/2}/2p_{1/2}$) and 3:2 ($3d_{5/2}/3d_{3/2}$). Due to the ultimate energy resolution and the presence of the spectra dominated by a single doublet, we were able to derive the initial setting for the respective parameters directly from the spectra. The resulting accuracy of the binding energies (BE) and fwhm's reported here is 0.04−0.05 eV. These values are noticeably lower than the ultimate accuracy of the experimental setup (see, e.g., ref 64), but mostly reflect the distribution of the resulting fit parameters over the spectra of different samples.

2.3. Time-of-Flight Secondary Ion Mass Spectrometry (ToF-SIMS). ToF-SIMS analyses were performed using a TOF SIMS IV (ION TOF Inc.). Briefly, the instrument consists of a load lock, a preparation/metal-deposition chamber, and an analysis chamber, each separated by a gate valve. The primary Bi^+ ions were accelerated to 25 keV and contained in a 150 nm diameter probe beam, which was rastered over a (100 × 100) μm^2 area during data acquisition. All spectra were acquired in the static SIMS regime using a total ion dose of 7×10^7 ions cm^{-2}. Under these circumstances less than 0.0001% of the top surface receives an ion impact. The species generated arise from an area no greater than 10 nm^2 and are remote from the next point of analytical impact. Thus the spectral information obtained arises from a surface which is undamaged, and is not due to ion-induced reactions. The secondary ions generated were extracted into a time-of-flight mass spectrometer and reaccelerated to 10 keV before reaching the detector.

For each SAM four samples were prepared and three areas on each sample were examined. The relative peak intensities were reproducible to within ±15% from sample to sample and ±10% from scan to scan.

2.4. Raman Scattering. Room-temperature Raman scattering spectra were collected using a Renishaw inVia Raman Microscope (Gloucestershire, GL12 8JR, U.K.) with a CCD detector. The instrument was arranged in a backscattering geometry configuration, $z(xy)\bar{z}$, where x, y, and z refer to the, [100], [010], and [001] directions, respectively. In this configuration, only the LO phonon mode is observable; the TO phonon mode is forbidden via selection rules.[65] Excitation was provided by the 514.0 nm line of an Ar^+ ion laser operating at 8.0 A and 10.0 mV. This

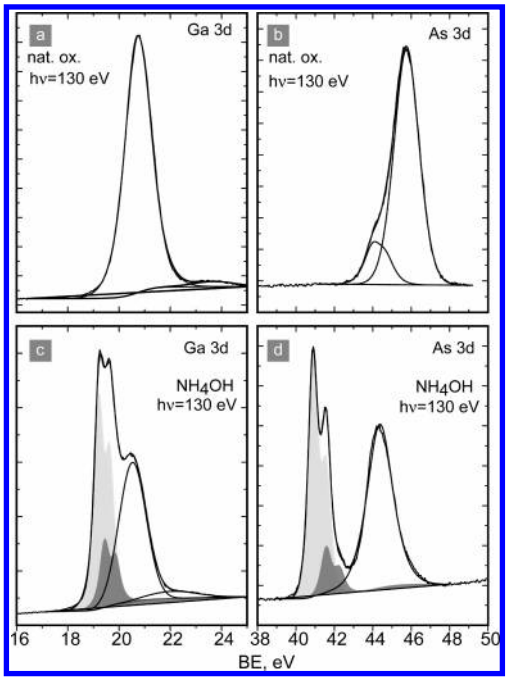

Figure 1. Ga 3d and As 3d HRXPS spectra of native (a and b) and freshly etched (c and d) GaAs (001) (see text for details). The spectra were acquired at a PE of 130 eV. A decomposition of distinct spectral features by doublets related to individual chemical species is shown. Ga 3d spectra: light gray, GaAs; gray, Ga oxide or the surface Ga 3d component. As 3d spectra: light gray, GaAs; gray, elementary As. The broad peaks at the high binding energy side of the shadowed doublets correspond to Ga and As oxides.

wavelength permits an optical penetration depth of $\sim 10^2$ nm,[16,66] which is larger than the doping region (∼10−40 nm[67]) for the highly doped GaAs wafers and results in excitation of both bulk and surface regions. All spectra were collected from the same wafer at different stages of treatments, under the same instrumental conditions, for easy comparison of the intrinsic changes in peak intensities as a function of surface treatment.

3. Results

3.1. HRXPS. To compare and reference the DDT and ODT monolayers on GaAs, samples of the native oxide and freshly etched GaAs(001) substrate were studied. All samples were freshly treated on site and placed immediately in the load-lock vacuum chamber of the analysis station. The native GaAs was rinsed sequentially with acetone, ethanol, and water, while the etched sample was sequentially treated with NH_4OH and water.

The Ga 3d and As 3d spectra, shown in Figure 1, were acquired at a photon energy of 130 eV, chosen to achieve a maximum surface sensitivity (the electron mean free path reaches its minimum value at kinetic energies of 50−100 eV).[68,69] The spectra are decomposed into individual spectral components. The derived parameters and the assignments of individual peaks are presented in Table 1.

The spectra of the native GaAs in Figure 1a,b show that the entire near-surface region of this sample is heavily oxidized. Only binding energy signatures related to Ga and As oxides are observed, whereas the signatures assigned to stoichiometric GaAs are not perceptible. However, most of the oxides can be removed by wet chemical etching, as follows from the spectra of the respective sample in Figure 1c,d. These spectra exhibit the pronounced emissions related to stoichiometric GaAs (light gray) and elemental arsenide (gray), even though the oxide-related features are still quite strong. The comparably high

TABLE 1: Parameters of Individual Emissions in the Ga 3d and As 3d Spectra in Figures 1 and 2[a]

core level	binding energy (eV)	assignment	fwhm (eV)	spin−orbit splitting (eV)	branching ratio
Ga $3d_{5/2}$	19.20 ± 0.05	GaAs	0.53 ± 0.05	0.43	3/2
	19.5 ± 0.1	Ga_2O_3 or surface Ga 3d component			
	>19.8	Ga oxides			
As $3d_{5/2}$	41.08 ± 0.03	GaAs	0.64 ± 0.05	0.69	3/2
	41.85 ± 0.05	elementary As (As^0)			
	42.35 ± 0.05	As−S			
	>43.0	As oxides			

[a] The parameters were derived from a self-consistent fitting procedure. The errors reflect the scattering of the fitting parameters between the spectra for different samples and different PEs. The assignments were performed in accordance with refs 12, 13, 23, 45, and 70−74.

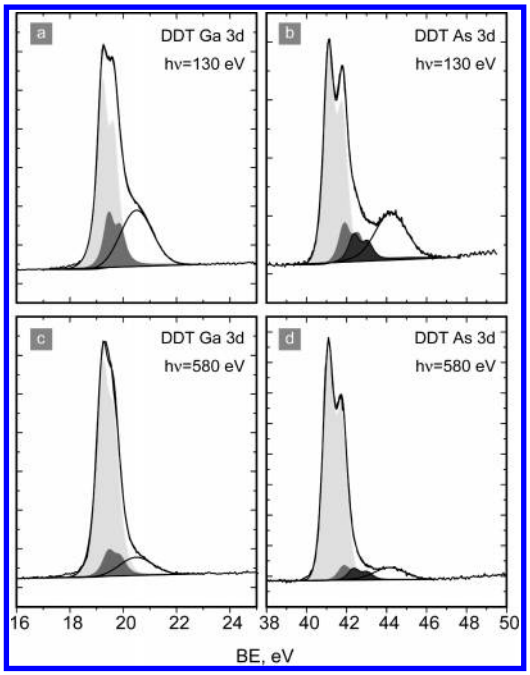

Figure 2. Ga 3d and As 3d HRXPS spectra of DDT/GaAs. The spectra were acquired at PEs of 130 (a and b) and 580 eV (c and d) and are dominated by contributions from the sample surface and bulk, respectively. A decomposition of distinct spectral features by doublets related to individual chemical species is shown. Ga 3d spectra: light gray, GaAs; gray, Ga oxide or surface Ga 3d component. As 3d spectra: light gray, GaAs; gray, elementary As; black, S−As. The shoulders at the high binding energy side of the shadowed doublets correspond to Ga and As oxides.

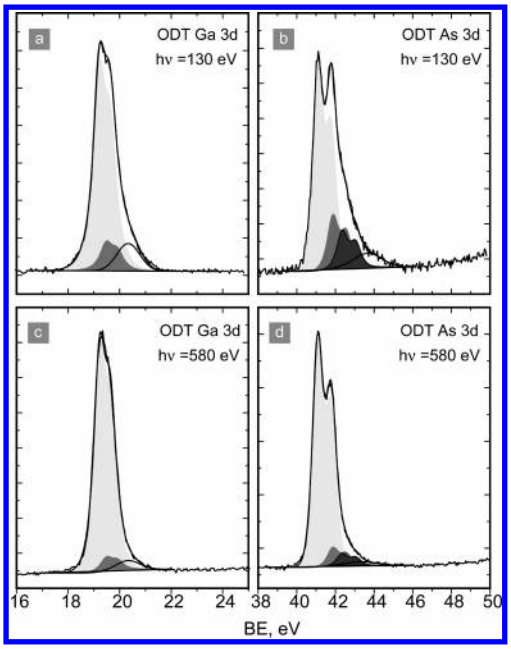

Figure 3. Ga 3d and As 3d HRXPS spectra of ODT/GaAs. The spectra were acquired at PEs of 130 (a and b) and 580 eV (c and d) and are dominated by contributions from the sample surface and bulk, respectively. A decomposition of distinct spectral features by doublets related to individual chemical species is shown. Ga 3d spectra: light gray, GaAs; gray, Ga oxide or surface Ga 3d component. As 3d spectra: light gray, GaAs; gray, elementary As; black, S−As. The shoulders at the high binding energy side of the shadowed doublets correspond to Ga and As oxides.

intensity of the latter features represents oxidation of the freshly etched sample during its mounting on the sample holder in the load-lock chamber of the spectrometer. This spectrum is similar to that of residual oxide species previously observed on NH_4-OH etched GaAs(001) surfaces[50,51] and also intrinsically present on the surface prior to SAM formation.[75]

The Ga 3d and As 3d spectra of DDT/GaAs and ODT/GaAs are presented in Figures 2 and 3, respectively. These spectra were acquired at photon energies of 130 eV (panels a and b) and 580 eV (panels c and d), to monitor the changes in the intensity of the individual spectral component by going from the sample surface to its bulk. At these photon energies, the effective sampling depth ($\approx 3\lambda$) is about 18 Å (130 eV) and 32 Å (580 eV),[68,69] with a larger spectral weight for the contributions from the topmost layers. In the same manner as the spectra in Figure 1, the spectra in Figures 2 and 3 are decomposed into individual spectral components, with the parameters and assignments given in Table 1.

The weaker contributions from Ga and As oxides in the spectra in Figures 2 and 3 compared to Figure 1 demonstrate that the formation of SAMs results in a significant decrease in the oxidation of the GaAs substrate compared to the NH_4OH etched GaAs surface. Also, this comparison shows that the DDT and ODT SAMs are able to protect the underlying GaAs substrate from oxidation and degradation; otherwise an even stronger degree of oxidation than in the case of the freshly etched samples could be expected, since both the DDT and ODT SAMs on GaAs were stored for several days before HRXPS measurements were made. Furthermore, protection of the GaAs surface by the ODT layer is more effective than that by the DDT layer, since the signatures related to oxides are much weaker for the ODT SAMs on GaAs. It appears that ODT and DDT molecules clean the GaAs surface of oxides and contamination during the SAM formation. This "cleaning" is more effective for the ODT molecules, which results in a better quality SAM.

The Ga 3d and As 3d spectra of DDT/GaAs and ODT/GaAs are dominated by peaks related to the stoichiometric GaAs (light gray) and elemental As (gray). The spectral weight of the former increases even further by going to 580 eV (panels c and d in Figure 2 and Figure 3), which suggests that both elemental As and residual Ga and As oxides are located at the substrate surface (i.e., at the SAM−GaAs interface).

In addition to the above mentioned emissions and the surface component of the Ga 3d spectrum (possibly also Ga_2O_3), a new doublet (black) assigned to As bonded to the thiol headgroup

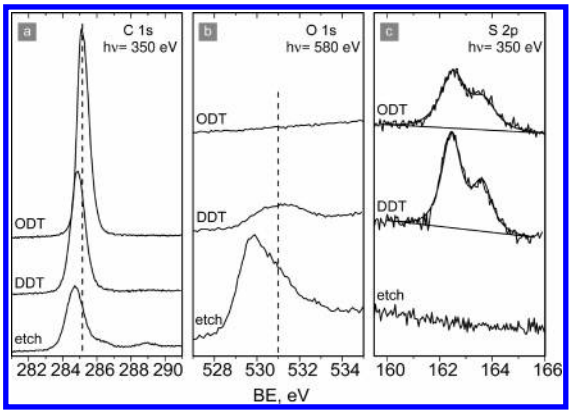

Figure 4. C 1s (a), O 1s (b), and S 2p (c) HRXPS spectra of freshly etched bare GaAs (bottom curves), DDT/GaAs (middle curves), and ODT/GaAs (top curves). A fit of S 2p spectra by a S $2p_{3/2,1/2}$ doublet is shown (see text for details).

of DDT or ODT is also observed at 42.35 eV and assigned to the As−S species. As expected, the intensity of this doublet decreases with increasing sampling depth, as follows from the comparison of the 130 and 580 eV spectra in Figures 2 and 3. In contrast to the As 3d spectra, the decomposition of the Ga 3d spectra of DDT/GaAs and ODT/GaAs does not require an introduction of an additional (with respect to the bare substrate) doublet related to the Ga−S species. Nevertheless, the existence of such a doublet, even though very weak, cannot be completely excluded, due to an ambiguity of the spectra fitting in the relevant BE region.[76]

The formation of the thiolate bond to the substrate is also exhibited in the S 2p spectra of DDT/GaAs and ODT/GaAs, presented in Figure 4 along with the C 1s and O 1s spectra for these samples and compared with the data for the freshly etched GaAs substrate. In the S 2p spectra of DDT/GaAs and ODT/GaAs, a single doublet at a characteristic binding energy of about 162.5 eV (S $2p_{3/2}$) is observed.[77] This energy coincides with the analogous values observed previously for SAMs of non-substituted and 4′-substituted biphenylthiolates on GaAs.[26,45,46] It is also noted that the value of 162.5 eV is noticeably higher than that for the thiol-derived SAMs on noble metal substrates (162.0 eV),[62,78−80] which is presumably related to the screening of the photoemission hole by the substrate electrons in the case of metal. The S $2p_{3/2}$ and S $2p_{1/2}$ components in the spectra of DDT/GaAs and ODT/GaAs are noticeably broader (0.9−1.1 eV) than the analogous peaks for alkanethiolates on noble metal substrates (0.55−0.6 eV),[62] presumably due to inhomogeneous site broadening effects.[81]

The conclusions derived from the Ga 3d, As 3d, and S 2p data are supported by the respective C 1s and O 1s spectra in Figure 4. The C 1s spectrum of ODT/GaAs exhibits a single pronounced peak at a BE of 285.2 eV, which is somewhere between the analogous values observed for ODT/Au (284.95 eV)[82] and ODT/Ag (285.26 eV).[82] No traces of oxidized carbon species could be found. Also, there is almost no signal in the O 1s spectrum of ODT/GaAs, which correlates with an extremely low intensity of the oxide-related features in the respective Ga 3d and As 3d spectra acquired at the same photon energy (580 eV).

The BE position of the C 1s peak for DDT/GaAs is somewhat lower, 284.9 eV, than that for ODT/GaAs and is similar to that for DDT/Au (284.87 eV).[82] Also, this peak is broader than that for ODT/GaAs (fwhm = 0.96 eV vs 0.77 eV) and indicates that the DDT film is less homogeneous. In addition, the intensity of the C 1s signal for DDT SAMs is a factor of 1.75 lower

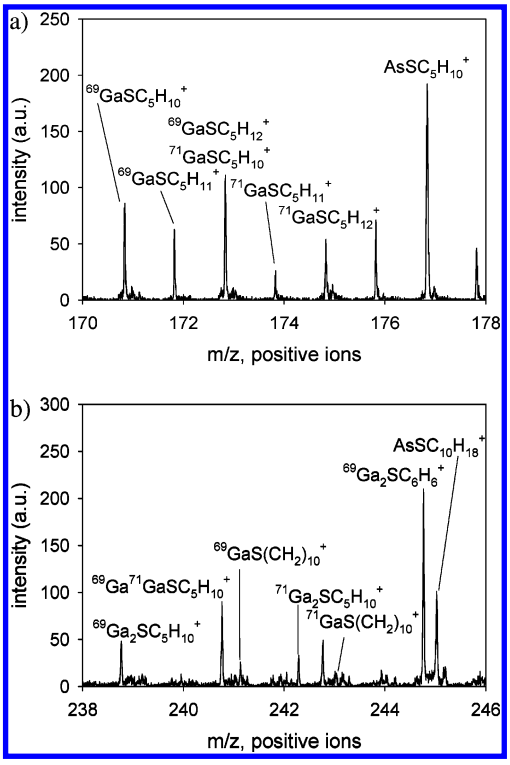

Figure 5. Positive ion mass spectra of (a) ODT and (b) DDT adsorbed on GaAs(001).

than for the ODT SAMs. This suggests a lower packing density of the DDT SAM even after consideration of the differences in the chain lengths of the DDT and ODT molecules on the C 1s signal. Despite the lower packing density, the DDT film on GaAs shows little contamination in comparison to the analogous spectrum for the freshly etched GaAs, in which there is pronounced oxidized C and the main emission is observed at 284.7 eV. The lower packing density of the DDT SAM has also been noted in a recent study.[25]

The O 1s spectrum of DDT/GaAs exhibits a pronounced, although small, signal, which correlates with the noticeable oxide-related features in the respective Ga 3d and As 3d spectra. The difference compared to the O 1s spectra for the freshly etched bare GaAs is, however, obvious, in terms of both spectral shape and intensity, which supports our previous statement about the protection effect of alkanethiolate SAMs.

3.2. ToF-SIMS. The ToF-SIMS spectra of ODT and DDT adsorbed on GaAs are similar to the spectra observed for these SAMs adsorbed on Au.[83−88] No features in the mass spectra were observed that indicate the presence of oxidized alkanethiolates such as SO_x^- ($x = 1-4$).[87−89] Prominent ions in the positive ion mass spectra include $(CH_2)_x^+$, $(CH_2)CH^+$, $CH_3(CH_2)_x^+$, $S(CH_2)_x^+$, Ga^+, and As^+. The positive ion mass spectra also exhibit a number of higher mass ions containing both Ga and As such as $Ga_xS_y(CH_2)_z^+$, $As_xS_y(CH_2)_z^+$, $Ga_xAs_yS_z(CH_2)_a^+$, $Ga_xS_y(CH_2)_zCH_3^+$, and $As_xS_y(CH_2)_z^+$. Figure 5 includes representative regions of the positive ion mass spectra of both ODT (Figure 5a) and DDT (Figure 5b) showing these types of ions. In the ODT positive ion mass spectra we also observe ions containing intact adsorbate ions, and Ga or As, such as GaM^+ and AsM^+ (Figure 6). In the negative ion mass spectra the prominent ions are $Ga_xS_y^-$, $As_xS_y^-$, $Ga_xS_y(CH_2)_z^-$, and $As_xS_y(CH_2)_z^-$. The presence of Ga-, As-, and S-containing ions in both the positive and negative ion mass spectra indicate that there are both As−S and Ga−S bonds present on the surface, though the data cannot distinguish the relative amounts because of

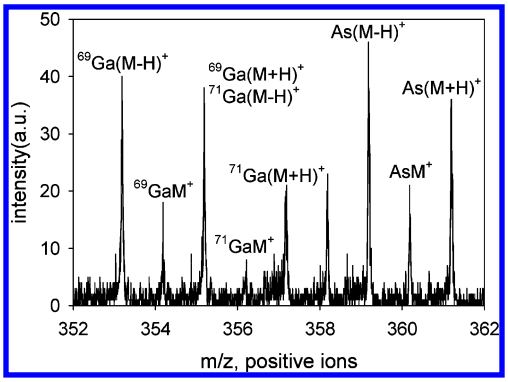

Figure 6. Positive ion mass spectra of ODT SAMs adsorbed on GaAs-(001) showing both GaM^+ and AsM^+, where M is the intact adsorbed molecular ion.

unknown ionization cross sections and associated matrix effects. We note that in the high-mass negative ion mass spectra (m/z > 520) of DDT, there is a series of cluster ions of the form $Ga_xS_y^-$ and $As_xS_y^-$, where $x > 4$, which are not observed in the ODT spectrum (see the Supporting Information). These ions could not be uniquely identified, and their presence suggests that the ODT and DDT SAMs may have a slightly different structure on the GaAs surface.

3.3. Raman Scattering. Since previous reports have demonstrated the use of intensity shifts in the LO lattice phonon spectrum of treated GaAs surfaces to detect changes in the surface electronic states,[16,19,90−92] we applied Raman scattering measurements to discern the effect of a direct thiolate bond from ODT and DDT monolayers on the surface electronic states of our samples. In general, three peaks can be observed in the Raman spectra of n-type GaAs wafers:[93] the L_- and L_+ coupled plasmon−phonon modes and the LO phonon mode, which is decoupled from the free carriers in the surface depletion layer. For highly doped samples, the L_- mode is more phonon-like with a frequency close to the TO phonon. Conversely, the L_+ mode is regarded as more plasmon-like in character and the frequency of this mode is a function of the dopant density ($\sqrt{N_e}$).[67] On the two types of native GaAs wafers measured in this study, the L_-, LO, and L_+ modes were observed at 269, 290, and 548 cm^{-1} for $N_e = 2.7 \times 10^{18}$ cm^{-3} and 270, 290, and 504 cm^{-1} for $N_e = 1.1 \times 10^{18}$ cm^{-3} doped samples, respectively. The position of the L_- and LO modes did not shift after monolayer formation, consistent with the expected invariance of the GaAs phonon character.

Since the intensity of the LO phonon mode varies with the depth of the surface depletion layer while the L_- mode is relatively invariant, the ratio of these mode intensities can reveal the effect of each surface treatment on the electronic passivation of the GaAs surface.[16,19,94] A summary of the measured (I_{LO}/I_{L_-}) values for the starting GaAs(001) substrate with native oxide, the corresponding NH_4OH etched surface, and the final ODT and DDT SAMs, taken from the spectra in Figure 7, is presented in Table 2. The table also shows comparison data taken from ref 19.

While some change in I_{LO}/I_{L_-} is observed between our starting oxide covered wafers and the NH_4OH etched surfaces, no significant changes are seen for the ODT or DDT functionalized surfaces for either of the two dopant densities. In contrast, the earlier data of Dorsten and co-workers,[19] summarized in the bottom row of Table 2, shows an ∼20% decrease in the I_{LO}/I_{L_-} ratio in going from the oxide-covered wafer to the ODT SAM. The authors interpreted this result in terms of a 25% reduction in the thickness (width) of the surface depletion layer compared

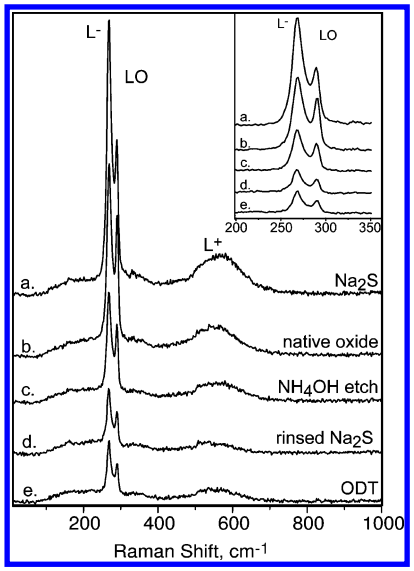

Figure 7. Comparison of Raman spectra of a GaAs(001) wafer n^+ doped at ∼2.7×10^{18} cm^{-3} shown for (a) $Na_2S{\cdot}H_2O$ functionalized wafer in comparison with (b) native oxide, (c) freshly etched NH_4OH surface, (d) $Na_2S{\cdot}H_2O$ functionalized wafer after rinsing with H_2O and ethanol, and (e) ODT functionalized surface.

to the native oxide surface.[19] Since no independent characterization of the SAM was reported, no direct correlations of the Raman results with interfacial structure and chemistry can be made. In the present case of thoroughly characterized SAMs, we conclude that formation of an oxide-free, uniform (molecule)−S−[GaAs(001)] interface exhibiting predominant As−S bonding and highly organized chains does not lead to any significant changes in the Raman spectra, and thereby to the surface electronic properties as manifested in the LO spectra. For the NH_4OH etched surface, no increase in the LO mode is observed for the $N_e = 2.7 \times 10^{18}$ cm^{-3} sample but an increase is observed for the $N_e = 1.1 \times 10^{18}$ cm^{-3} sample, though the effect is transient (I_{LO}/I_{L_-} returns to the starting native oxide value within 30 min).

As an independent check of our experimental methods and analysis, we prepared a inorganic sulfide treated sample. A $N_e = 2.7 \times 10^{18}$ cm^{-3} oxide covered wafer was etched with NH_4OH and then spin-coated with an aqueous $Na_2S{\cdot}H_2O$ solution, a procedure previously shown to have a dramatic affect on the surface electronic states of GaAs.[4,6,16] The data in Figure 7 show that after treatment the I_{LO}/I_{L_-} ratio decreases ∼20% from the starting native oxide value, comparable to the ∼27−35% I_{LO}/I_{L_-} ratio decrease reported previously.[16] Further, as previously observed,[16] the surface treatment effect is short-lived:[95] after rinsing with H_2O and ethanol, the I_{LO}/I_{L_-} ratio quickly returns within minutes to the original native oxide value (see Figure 7). Given the known variability of these inorganic sulfide surface treatments, our experiment agrees well with the reports.

4. Discussion

A combination of HRXPS and ToF-SIMS measurements show that the interfaces of ODT and DDT SAMs on GaAs-(001) substrates consist of direct thiolate bonds to the bare GaAs surface. The HRXPS data reveal dominant As−S bonding, while the ToF-SIMS data show evidence that some fraction of Ga−S bonds also exists. The presence of Ga−S bonds is expected thermochemically since Ga−S bonds are typically more energetically favorable than As−S bonds.[34−37,39] This would be consistent with what has been observed on other III−V (001) surfaces, where the thiolate species bond predominantly to the

TABLE 2: Changes in LO and L$_-$ Phonon Mode Intensities as a Function of Surface Treatment of n$^+$ GaAs(001)

	I_{LO}/I_{L_-} values[a]				
doping (n) level, cm^{-3}	native oxide	NH_4OH etch[b]	ODT SAM	DDT SAM	Na_2S[c]
1.1×10^{18}	0.96 ± 0.00	1.26 ± 0.02	1.02 ± 0.05	1.00 ± 0.04	
2.7×10^{18}	0.76 ± 0.00	0.74 ± 0.02	0.74 ± 0.03	0.74 ± 0.01	0.61 ± 0.06
3.0×10^{18} [d]	~ 1.33[d]		~ 1.04[d]		

[a] The errors are the standard deviations observed for a minimum of three samples with a minimum of three measurements for each sample. [b] These values represent the initial I_{LO}/I_{L_-} ratio within the first 5 min of sample etching. Within 30 min, the I_{LO}/I_{L_-} ratio returned to the initial native oxide ratios. [c] These experiments were only performed on the 2.7×10^{18} cm^{-3} doped wafers. [d] For comparison purposes, these values are taken from Figure 1 in ref 19.

group III atoms.[96−101] For example, in the case of SAMs of alkanethiols formed on InP, only In−S bonds have been observed[96,97] and inorganic sulfide treated InAs surfaces show a predominance of In−S bonds, with small fractions of As−S bonds proposed to exist at defect and step edge sites.[98−101] In the present case, however, the dominance of As−S bonds suggests that the monolayer assembly process may be driven in a significant part by kinetic competitions.

The presence of both Ga−S and As−S bonds has important structural ramifications. Given our earlier conclusions for the ODT case that the average molecule spacing is incommensurate with any simple spacing on the intrinsic (001) square lattice surface,[24,102] it seems reasonable that some disruption of the intrinsic lattice arises on SAM formation with the possibility for the presence of both As and Ga atoms, relative to the ideal cases of all As or all Ga surface planes. We note that in recent work we have observed ordered ODT SAMs to form on GaAs-(011) surfaces, which have equal numbers of As and Ga atoms, and also on the (111A) surfaces, which are terminated exclusively by Ga atoms.[103] Thus it appears that driving forces such as maximum density molecular packing may be important in the film assembly process and the substrate composition and lattice arrangements might be overridden by other factors.

The HRXPS measurements show differences in detail between the two SAMs. While the ODT SAM exhibits C 1s peak positions and line shapes similar to those of ODT/Au and ODT/Ag SAMs,[82] the DDT SAM exhibits a broader C 1s peak shifted to lower BE, suggestive of a more nonuniform film. The nonproportionally lower peak intensity of the C 1s signal for the DDT SAM also suggests a lower packing density for this SAM, consistent with our recent data which show that the ODT SAMs form with a higher degree of conformational ordering of the chains than the DDT case.[104] These differences have been interpreted on the basis of the total number of intermolecular interactions between the chains that are available to drive self-organization compared to the influences of molecule−substrate interactions.[104,105]

These structural differences are consistent with the differences in the presence of oxide in the SAM interfaces. For the freshly NH_4OH etched GaAs substrate in a condition similar to that just prior to thiolate immersion, the HRXPS spectra show significantly lower quantities of oxides compared with the native oxide, but the spectra of the ordered ODT SAM show virtually no observable oxide, consistent with a dense chain structure that could prevent penetration of ambient O_2. In comparison, the more disordered DDT SAM contains small amounts of oxide species, though far less than the etched substrate, suggestive of easier O_2 penetration. Further, these data suggest that removal of residual substrate oxide species after both DDT and ODT SAM formation occurs by a "cleaning" action of the alkanethiol molecules, possibly involving exchange reactions of S for O species and sacrificial reduction of inorganic oxide by thiols.[24] We note that in earlier reports of GaAs(001) surfaces treated with small inorganic chalcogenides it was suggested that the chalcogenide species bond to the surface via an exchange reaction.[106,107]

It is interesting that only one peak in the S 2p spectra (162.5 eV) is observed for both the ODT and DDT SAMs at a binding energy which is the same as that observed for 4′-substituted biphenylthiolate SAMs formed on GaAs(001) surfaces in experiments using HCl etching of the substrates.[46] This comparison suggests that similar interfacial chemistry might exist for all organothiolate molecules bound to GaAs(001), regardless of the etching chemistry.

Finally, based on Raman spectroscopic characterization of the LO phonons, no changes in the GaAs surface electronic states from SAM formation are observed, despite the presence of direct thiolate bonding to the bare semiconductor, though effects are observed on simple inorganic sulfide treatment of bare GaAs samples, consistent with previous reports.[16,90,108] From this we conclude that formation of a well-organized ODT/GaAs(001) SAM with direct thiolate−substrate bonding is not sufficient in itself to cause significant changes in the surface electronic states. This is an important consideration based on the longstanding interest in using surface treatments for precise control of the surface electronic properties.[1,2]

One way to understand this behavior is on the basis that the alkanethiolate adsorbate species, even with the densest possible packing, cannot bind to all the Ga and/or As atoms in the intrinsic (001) lattice, thus leaving a significant fraction of the III−V atoms unbound and potentially able to act as surface traps.[109] For example, the average lateral molecular spacing of 4.5 Å for the ODT SAM (based on the measured average 14° chain tilt angle; this spacing value is also close to the interchain distance of hydrocarbon crystals[110]) is larger than the 4.00 Å nearest-neighbor (NN) spacings of the atoms in the intrinsic square GaAs(001) surface lattice, thus preventing occupation of an NN superlattice. The next larger superlattice involves the next-nearest-neighbor spacing (NNN) [$c(2\times2)$ superlattice] at an ideal distance of 5.65 Å, which leaves half of the substrate surface atoms unterminated by molecules. While our current understanding of these SAMs involves some disruption (reconstruction) of the intrinsic square (001) lattice, the main point is that it is very unlikely that the final lattice would exist in such a way that all the substrate atoms were terminated by bonding to a molecule given the large differences in the molecular and intrinsic lattice spacings. Determination of the real coverage of the ODT or DDT monolayers, for example, through absolute intensity calibration HRXPS measurements or through an independent technique such as scanning probe or diffraction methods, in combination with these results would lead to a clearer understanding of the interfacial bonding sites.

Extending this picture to the case of electronic passivation by inorganic sulfide treatment, since the covalent radius of sulfur (1.02 Å) is close to the covalent radii of Ga and As atoms (1.26 and 1.19 Å, respectively), the inorganic sulfide species in

principle could be chemisorbed on the GaAs lattice structure to terminate a larger fraction of the substrate atoms than might be possible for alkanethiolate SAMs. This point also possibly relates to the contrasting invariance in the (LO/L_-) intensity ratio for our ODT SAM compared to the starting GaAs sample and the previous report of an ∼20% change in the ratio for an ODT SAM made by a melt deposition procedure.[19] We cannot directly conclude the basis for this difference since the structure for the SAM in the earlier report is uncertain, but it is possible that shifts in the interfacial bonding states could contribute. The reported work[19] was done using deposition of the etched GaAs wafer in pure molten ODT at 100 °C, compared to our present use of dilute solution conditions at ambient temperature. It would not be unexpected that the considerable change in processing temperature and solute concentration would produce different states of the underlying lattice structure and atom composition. Further, possibilities such as adsorbate decomposition to small amounts of inorganic sulfur species at the higher temperatures could result in an additional mechanism to terminate unbonded substrate lattice sites.

5. Conclusions

In conclusion, it has been shown that DDT and ODT SAMs form direct thiolate bonds to the GaAs(001) surface with dominant As−S bonding and some fraction of Ga−As bonding. While formation of both SAMs is successful in removing initial substrate oxide and substantially effective in preventing subsequent interface oxide regrowth, the ODT SAMs are significantly more effective in keeping oxide-free interfaces. These differences can be understood on the basis of the more dense packing of the ODT SAM which can prevent ambient O_2 diffusion through the film. Finally, formation of densely packed SAMs with oxide-free interfaces and direct thiolate−substrate bonding appears not to be effective in modifying the surface electronic states of the GaAs(001) samples as determined by LO phonon spectral analysis.

Acknowledgment. The authors acknowledge support from DARPA and from the NSF-funded Pennsylvania State University Center for Nanoscale Science (MRSEC DMR-0080019).

Supporting Information Available: ToF-SIMS: positive ion mass spectra of DDT, $m/z = 0-800$; negative ion mass spectra of DDT, $m/z = 0-800$; positive ion mass spectra of ODT, $m/z = 0-800$; negative ion mass spectra of ODT, $m/z = 0-800$. Additional Raman scattering spectra. This material is available free of charge via the Internet at http://pubs.acs.org.

References and Notes

(1) Seker, F.; Meeker, K.; Kuech, T. F.; Ellis, A. B. *Chem. Rev.* **2000**, *100*, 2505−2536.

(2) Bessolov, V. N.; Lebedev, M. V. *Semiconductors* **1998**, *32*, 1141−1156.

(3) Lebedev, M. V. *Prog. Surf. Sci.* **2002**, *70*, 153−186.

(4) Yablonovitch, E.; Sandroff, C. J.; Bhat, R.; Gmitter, T. *Appl. Phys. Lett.* **1987**, *51*, 439−441.

(5) Skromme, B. J.; Sandroff, C. J.; Yablonovitch, E.; Gmitter, T. *Appl. Phys. Lett.* **1987**, *51*, 2022−2024.

(6) Sandroff, C. J.; Nottenburg, R. N.; Bischoff, J. C.; Bhat, R. *Appl. Phys. Lett.* **1987**, *51*, 33−35.

(7) Lu, E. D.; Zhang, F. P.; Xu, S. H.; Yu, X. J.; Xu, P. S.; Han, Z. F.; Xu, F. Q.; Zhang, X. Y. *Appl. Phys. Lett.* **1996**, *69*, 2282−2284.

(8) Lu, E. D.; Xu, F. Q.; Sun, Y. M.; Pan, H. B.; Zhang, F. P.; Xu, P. S.; Zhang, X. Y. *J. Electron Spectrosc. Relat. Phenom.* **1999**, *103*, 429−432.

(9) Yang, G. H.; Zhang, Y.; Kang, E. T.; Neoh, K. G.; Huang, W.; Teng, J. H. *J. Phys. Chem. B* **2003**, *107*, 8592−8598.

(10) Donev, S.; Brack, N.; Paris, N. J.; Pigram, P. J.; Singh, N. K.; Usher, B. F. *Langmuir* **2005**, *21*, 1866−1874.

(11) Singh, N. K.; Doran, D. C. *Surf. Sci.* **1999**, *422*, 50−64.

(12) Lunt, S. R.; Ryba, G. N.; Santangelo, P. G.; Lewis, N. S. *J. Appl. Phys.* **1991**, *70*, 7449−7465.

(13) Lunt, S. R.; Santangelo, P. G.; Lewis, N. S. *J. Vac. Sci. Technol., B* **1991**, *9*, 2333−2336.

(14) Carpenter, M. S.; Melloch, M. R.; Dungan, T. E. *Appl. Phys. Lett.* **1988**, *53*, 66−68.

(15) Carpenter, M. S.; Melloch, M. R.; Lundstrom, M. S.; Tobin, S. P. *Appl. Phys. Lett.* **1988**, *52*, 2157−2159.

(16) Farrow, L. A.; Sandroff, C. J.; Tamargo, M. C. *Appl. Phys. Lett.* **1987**, *51*, 1931−1933.

(17) Sheen, C. W.; Shi, J. X.; Martensson, J.; Parikh, A. N.; Allara, D. L. *J. Am. Chem. Soc.* **1992**, *114*, 1514−1515.

(18) Nakagawa, O. S.; Ashok, S.; Sheen, C. W.; Martensson, J.; Allara, D. L. *Jpn. J. Appl. Phys. Part 1* **1991**, *30*, 3759−3762.

(19) Dorsten, J. F.; Maslar, J. E.; Bohn, P. W. *Appl. Phys. Lett.* **1995**, *66*, 1755−1757.

(20) Remashan, K.; Bhat, K. N. *Thin Solid Films* **1999**, *342*, 20−29.

(21) Ye, S.; Li, G. F.; Noda, H.; Uosaki, K.; Osawa, M. *Surf. Sci.* **2003**, *529*, 163−170.

(22) Adlkofer, K.; Tanaka, M.; Hillebrandt, H.; Wiegand, G.; Sackmann, E.; Bolom, T.; Deutschmann, R.; Abstreiter, G. *Appl. Phys. Lett.* **2000**, *76*, 3313−3315.

(23) Adlkofer, K.; Tanaka, M. *Langmuir* **2001**, *17*, 4267−4273.

(24) McGuiness, C. L.; Shaporenko, A.; Mars, C. K.; Uppili, S.; Zharnikov, M.; Allara, D. L. *J. Am. Chem. Soc.* **2006**, *128*, 5231−5243.

(25) Nesher, G.; Vilan, A.; Cohen, H.; Cahen, D.; Amy, F.; Chan, C.; Hwang, J. H.; Kahn, A. *J. Phys. Chem. B* **2006**, *110*, 14363−14371.

(26) Adlkofer, K.; Shaporenko, A.; Zharnikov, M.; Grunze, M.; Ulman, A.; Tanaka, M. *J. Phys. Chem. B* **2003**, *107*, 11737−11741.

(27) Adlkofer, K.; Eck, W.; Grunze, M.; Tanaka, M. *J. Phys. Chem. B* **2003**, *107*, 587−591.

(28) Krapchetov, D. A.; Ma, H.; Jen, A. K. Y.; Fischer, D. A.; Loo, Y. L. *Langmuir* **2005**, *21*, 5887−5893.

(29) Li, W. J.; Kavanagh, K. L.; Matzke, C. M.; Talin, A. A.; Leonard, F.; Faleev, S.; Hsu, J. W. P. *J. Phys. Chem. B* **2005**, *109*, 6252−6256.

(30) Hsu, J. W. P.; Lang, D. V.; West, K. W.; Loo, Y. L.; Halls, M. D.; Raghavachari, K. *J. Phys. Chem. B* **2005**, *109*, 5719−5723.

(31) Hsu, J. W. P.; Loo, Y. L.; Lang, D. V.; Rogers, J. A. *J. Vac. Sci. Technol., B* **2003**, *21*, 1928−1935.

(32) Xue, Q. K.; Hashizume, T.; Sakurai, T. *Prog. Surf. Sci.* **1997**, *56*, 1−131.

(33) Ranke, W.; Jacobi, K. *Prog. Surf. Sci.* **1981**, *10*, 1−52.

(34) Scimeca, T.; Muramatsu, Y.; Oshima, M.; Oigawa, H.; Nannichi, Y. *Phys. Rev. B* **1991**, *44*, 12927−12932.

(35) Ohno, T.; Shiraishi, K. *Phys. Rev. B* **1990**, *42*, 11194−11197.

(36) Lebedev, M. V.; Mayer, T.; Jaegermann, W. *Surf. Sci.* **2003**, *547*, 171−183.

(37) Medvedev, Y. V. *Appl. Phys. Lett.* **1994**, *64*, 3458−3460.

(38) Sandroff, C. J.; Hegde, M. S.; Farrow, L. A.; Chang, C. C.; Harbison, J. P. *Appl. Phys. Lett.* **1989**, *54*, 362−364.

(39) Spindt, C. J.; Liu, D.; Miyano, K.; Meissner, P. L.; Chiang, T. T.; Kendelewicz, T.; Lindau, I.; Spicer, W. E. *Appl. Phys. Lett.* **1989**, *55*, 861−863.

(40) Lu, Z. H.; Graham, M. J.; Feng, X. H.; Yang, B. X. *Appl. Phys. Lett.* **1993**, *62*, 2932−2934.

(41) Yuan, Z. L.; Ding, X. M.; Hu, H. T.; Li, Z. S.; Yang, J. S.; Miao, X. Y.; Chen, X. Y.; Cao, X. A.; Hou, X. Y.; Lu, E. D.; Xu, S. H.; Xu, P. S.; Zhang, X. Y. *Appl. Phys. Lett.* **1997**, *71*, 3081−3083.

(42) Heun, S.; Gregoratti, L.; Barinov, A.; Kaulich, B.; Rudolf, M.; Lazzarino, M.; Biasiol, G.; Bonanni, B.; Sorba, L. *Surf. Rev. Lett.* **2002**, *9*, 413−423.

(43) Lu, Z. H.; Graham, M. J. *Phys. Rev. B* **1993**, *48*, 4604−4607.

(44) Paget, D.; Bonnet, J. E.; Berkovits, V. L.; Chiaradia, P.; Avila, J. *Phys. Rev. B* **1996**, *53*, 4604−4614.

(45) Shaporenko, A.; Adlkofer, K.; Johansson, L. S. O.; Tanaka, M.; Zharnikov, M. *Langmuir* **2003**, *19*, 4992−4998.

(46) Shaporenko, A.; Adlkofer, K.; Johansson, L. S. O.; Ulman, A.; Grunze, M.; Tanaka, M.; Zharnikov, M. *J. Phys. Chem. B* **2004**, *108*, 17964−17972.

(47) Cho, Y.; Ivanisevic, A. *J. Phys. Chem. B* **2005**, *109*, 12731−12737.
(48) Hou, T.; Greenlief, M.; Keller, S. W.; Nelen, L.; Kauffman, J. F. *Chem. Mater.* **1997**, *9*, 3181−3186.
(49) William, R. E. *Gallium Arsenide Processing Techniques*; Artech House, Inc.: Dedham, MA, 1984.
(50) Chang, C. C.; Citrin, P. H.; Swartz, B. *J. Vac. Sci. Technol.* **1977**, *14*, 943−952.
(51) Aspnes, D. E.; Studna, A. A. *Appl. Phys. Lett.* **1985**, *46*, 1071−1073.
(52) Negri, F.; Bedel-Pereira, E. *J. Vac. Sci. Technol., B* **2002**, *20*, 2214−2218.
(53) Cohen, R.; Kronik, L.; Shanzer, A.; Cahen, D.; Liu, A.; Rosenwaks, Y.; Lorenz, J. K.; Ellis, A. B. *J. Am. Chem. Soc.* **1999**, *121*, 10545−10553.
(54) Ding, X. M.; Moumanis, K.; Dubowski, J. J.; Tay, L.; Rowell, N. L. *J. Appl. Phys.* **2006**, *99*, 54701.
(55) Band, I. M.; Kharitonov, Yu. I.; Trzhaskovskaya, M. B. *At. Data Nucl. Data Tables* **1979**, *23*, 443−505.
(56) Goldberg, S. M.; Fadley, C. S.; Kono, S. *J. Electron Spectrosc. Relat. Phenom.* **1981**, *21*, 285−363.
(57) Yeh, J. J.; Lindau, I. *At. Data Nucl. Data Tables* **1985**, *32*, 1−155.
(58) Wirde, M.; Gelius, U.; Dunbar, T.; Allara, D. L. *Nucl. Instrum. Methods Phys. Res., Sect. B* **1997**, *131*, 245−251.
(59) Jager, B.; Schurmann, H.; Muller, H. U.; Himmel, H. J.; Neumann, M.; Grunze, M.; Woll, C. *Z. Phys. Chem.* **1997**, *202*, 263−272.
(60) Heister, K.; Zharnikov, M.; Grunze, M.; Johansson, L. S. O.; Ulman, A. *Langmuir* **2001**, *17*, 8−11.
(61) Zharnikov, M.; Grunze, M. *J. Vac. Sci. Technol., B* **2002**, *20*, 1793−1807.
(62) Heister, K.; Zharnikov, M.; Grunze, M.; Johansson, L. S. O. *J. Phys. Chem. B* **2001**, *105*, 4058−4061.
(63) *Surface chemical analysis−X-ray photoelectron spectrometers−Calibration of the energy scales*; ISO 15472:2001: 2006.
(64) Heister, K.; Rong, H. T.; Buck, M.; Zharnikov, M.; Grunze, M.; Johansson, L. S. O. *J. Phys. Chem. B* **2001**, *105*, 6888−6894.
(65) Yu, P. Y.; Cardona, M. *Fundamentals of Semiconductors: Physics and Materials Properties*; Springer: New York, 2001.
(66) Aspnes, D. E.; Studna, A. A. *Phys. Rev. B* **1983**, *27*, 985−1009.
(67) Cardona, M.; Guntherodt, G. *Light Scattering in Solids IV*; Springer-Verlag: Berlin, 1984.
(68) Lindau, I.; Spicer, W. E. *J. Electron Spectrosc. Relat. Phenom.* **1974**, *3*, 409−413.
(69) Powell, C. J. *Surf. Sci.* **1974**, *44*, 29−46.
(70) Wagner, C. D.; Riggs, W. M.; Davis, L. E.; Moulder, J. F.; Muilenberg, J. E. *Handbook of X-ray Photoelectron Spectroscopy*; Perkin-Elmer Corp.: Eden Prairie, MN, 1979.
(71) Chang, S.; Vitomirov, I. M.; Brillson, L. J.; Rioux, D. F.; Kirchner, P. D.; Pettit, G. D.; Woodall, J. M. *J. Vac. Sci. Technol., B* **1991**, *9*, 2129−2134.
(72) Mao, D.; Kahn, A.; Lelay, G.; Marsi, M.; Hwu, Y.; Margaritondo, G.; Santos, M.; Shayegan, M.; Florez, L. T.; Harbison, J. P. *J. Vac. Sci. Technol., B* **1991**, *9*, 2083−2089.
(73) Shin, J.; Geib, K. M.; Wilmsen, C. W. *J. Vac. Sci. Technol., B* **1991**, *9*, 2337−2341.
(74) Moulder, J. F.; Stickle, W. E.; Sobol, P. E.; Bomben, K. D. *Handbook of X-ray Photoelectron Spectroscopy*; Perkin-Elmer Corp.: Eden Prairie, MN, 2006.
(75) The amount of time needed to mount the sample in the HRXPS spectrometer approximates the same amount of time taken to transfer samples from the NH_4OH solution into the glovebox where the sample is immediately exposed to a solution containing the SAM molecules.
(76) Since the doublet identified in the Ga 3d spectra as the Ga oxide or surface component has a binding energy similar to that expected for a Ga−S component, we coarsely evaluated the As 3d and Ga 3d HRXPS weighted intensities to determine the relative concentrations. If we assume that As and Ga are oxidized to the same extent, then a comparison of the Ga oxide intensity minus that of the As oxide intensity reveals that the upper limit for the Ga−S bonds is 10−20% of all S−As/Ga bonds while As−S bonds make up the remainder, 80−90%.
(77) The S 2p doublet was fit with a 2:1 intensity ratio and a spin−orbit splitting of 1.18 eV.
(78) Laibinis, P. E.; Whitesides, G. M.; Allara, D. L.; Tao, Y. T.; Parikh, A. N.; Nuzzo, R. G. *J. Am. Chem. Soc.* **1991**, *113*, 7152−7167.
(79) Himmelhaus, M.; Gauss, I.; Buck, M.; Eisert, F.; Woll, C.; Grunze, M. *J. Electron Spectrosc. Relat. Phenom.* **1998**, *92*, 139−149.
(80) Zharnikov, M.; Grunze, M. *J. Phys.: Condens. Matter* **2001**, *13*, 11333−11365.
(81) We note that the ODT S 2p peaks are slightly broader (1.1 eV) than those of the DDT peaks (0.9 eV) and this can only mean a larger inhomogeneity of the adsorption site geometry and exact bonding conditions for the ODT film. Since the ODT film is densely packed, it can result in a stochastical, noncommensurate placing of the thiolate headgroup on the GaAs surface, resulting in a larger inhomogeneity of the respective adsorption sites as compared to the less densely packed DDT film.
(82) Heister, K.; Johansson, L. S. O.; Grunze, M.; Zharnikov, M. *Surf. Sci.* **2003**, *529*, 36−46.
(83) Hooper, A.; Fisher, G. L.; Konstadinidis, K.; Jung, D.; Nguyen, H.; Opila, R.; Collins, R. W.; Winograd, N.; Allara, D. L. *J. Am. Chem. Soc.* **1999**, *121*, 8052−8064.
(84) Fisher, G. L.; Walker, A. V.; Hooper, A. E.; Tighe, T. B.; Bahnck, K. B.; Skriba, H. T.; Reinard, M. D.; Haynie, B. C.; Opila, R. L.; Winograd, N.; Allara, D. L. *J. Am. Chem. Soc.* **2002**, *124*, 5528−5541.
(85) Walker, A. V.; Tighe, T. B.; Cabarcos, O. M.; Reinard, M. D.; Haynie, B. C.; Uppili, S.; Winograd, N.; Allara, D. L. *J. Am. Chem. Soc.* **2004**, *126*, 3954−3963.
(86) Nagy, G.; Walker, A. V. *J. Phys. Chem. B* **2006**, *110*, 12543−12554.
(87) Hagenhoff, B.; Benninghoven, A.; Spinke, J.; Liley, M.; Knoll, W. *Langmuir* **1993**, *9*, 1622−1624.
(88) Tarlov, M. J.; Newman, J. G. *Langmuir* **1992**, *8*, 1398−1405.
(89) Hutt, D. A.; Leggett, G. J. *J. Phys. Chem.* **1996**, *100*, 6657−6662.
(90) Bessolov, V. N.; Lebedev, M. V.; Ivankov, A. F.; Bauhofer, W.; Zahn, D. R. T. *Appl. Surf. Sci.* **1998**, *133*, 17−22.
(91) Oconnor, G. M.; Mcdonagh, C. J.; Anderson, F. G.; Glynn, T. J.; Morgan, G. P.; Hughes, G. J.; Roberts, L.; Henry, M. O. *Appl. Surf. Sci.* **1991**, *50*, 312−316.
(92) Chen, X.; Si, X.; Malhotra, V. *J. Electrochem. Soc.* **1993**, *140*, 2085−2088.
(93) Data not shown; see the Supporting Information.
(94) Cardona, M. *Light Scattering Solids I*; Springer-Verlag: Berlin, 1983.
(95) We also note that, unlike the ODT and DDT SAMs, the $Na_2S\cdot 9H_2O$ treatment results in a nonuniform surface coating as seen by optical microscope imaging. Furthermore, initial Raman scans showed additional spurious peaks which gradually disappeared within 5−6 min of film formation and exposure to air. After approximately 5 min, the $Na_2S\cdot 9H_2O$ film reached a condition with invariant spectra. Our reported I_{LO}/I_{L} ratios were determined after this point. Details are given in the Supporting Information.
(96) Yamamoto, H.; Butera, R. A.; Gu, Y.; Waldeck, D. H. *Langmuir* **1999**, *15*, 8640−8644.
(97) Gu, Y.; Lin, Z.; Butera, R. A.; Smentkowski, V. S.; Waldeck, D. H. *Langmuir* **1995**, *11*, 1849−1851.
(98) Petrovykh, D. Y.; Sullivan, J. M.; Whitman, L. J. *Surf. Interface Anal.* **2005**, *37*, 989−997.
(99) Petrovykh, D. Y.; Long, J. P.; Whitman, L. J. *Appl. Phys. Lett.* **2005**, *86*, 242105.
(100) Petrovykh, D. Y.; Yang, M. J.; Whitman, L. J. *Surf. Sci.* **2003**, *523*, 231−240.
(101) Fukuda, Y.; Suzuki, Y.; Sanada, N.; Shimomura, M.; Masuda, S. *Phys. Rev. B* **1997**, *56*, 1084−1086.
(102) This interpretation is different from the commensurate monolayer structure suggested by Nesher et al. (see ref 25), where the thiolate molecules only bind to As atoms while the remaining Ga atoms are bound to interstitial oxygen atoms.
(103) McGuiness, C. L.; Blasini, D.; Masejewski, J. P.; Uppilin, S.; Cabarcos, O. M.; Smilgies, D.; Allara, D. L. Manuscript in preparation.
(104) McGuiness, C. L.; Blasini, D.; Masejewski, J. P.; Uppili, S.; Cabarcos, O. M.; Smilgies, D.; Allara, D.L. Manuscript in preparation.
(105) Schreiber, F. *Prog. Surf. Sci.* **2000**, *65*, 151−256.
(106) Chambers, S. A.; Sundaram, V. S. *J. Vac. Sci. Technol., B* **1991**, *9*, 2256−2262.
(107) Chambers, S. A.; Sundaram, V. S. *Appl. Phys. Lett.* **1990**, *57*, 2342−2344.
(108) We note that a recent report of photoluminescence experiments on long chain alkanethiolate SAMs prepared on GaAs(001) by ambient-temperature solution deposition concluded there were only very small effects of the SAMs on the surface electronic properties compared to the native oxide; see ref 54. Again, however, since no detailed characterization data of the interfacial bonding and SAM structures were available, and a different electronic surface probe was used, direct comparisons and structure−property correlations are problematic.
(109) Preliminary experiments with epitaxially grown Mn doped GaAs samples have shown that ODT SAMs do affect the surface electronic states of these surfaces, as evidenced by a ∼15−30% I_{LO}/I_{L} ratio decrease after SAM formation compared to the starting native oxide spectra. McGuiness, C. L.; Samarth, N.; Allara, D. L., unpublished results.
(110) Muller, A.; Lonsdale, K. *Acta Crystallogr.* **1948**, *1*, 129−131.